LBL-24506

Lawrence Berkeley Laboratory
UNIVERSITY OF CALIFORNIA

Presented at the XVIII International Symposium
on Multiparticle Dynamics,Tashkent, USSR,
September 8–12, 1987

Nuclear Breakup and Particle Densities in 200 A Gev – ^{16}0 Interactions with Emulsion Nuclei

EMU-01 Collaboration

September 1987

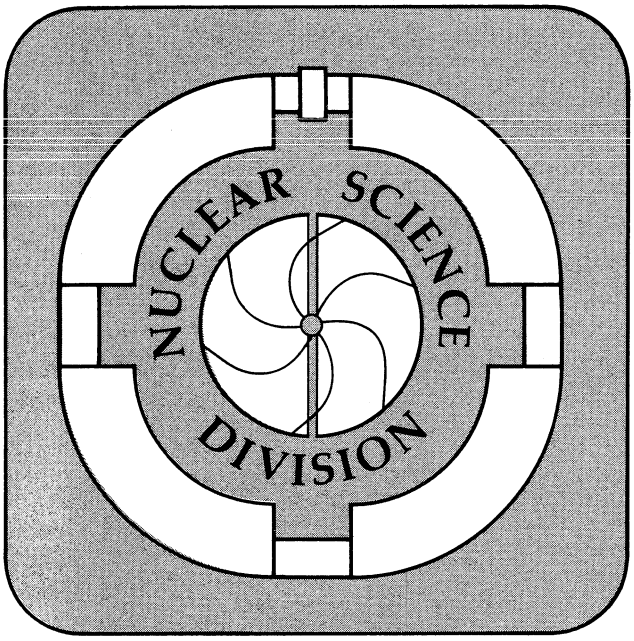

Prepared for the U.S. Department of Energy under Contract DE-AC03-76SF00098

Nuclear Breakup and Particle Densities in 200 A GeV - ^{16}O Interactions with Emulsion Nuclei

EMU-01 COLLABORATION:

M I Adamovich[9], Y A Alexandrov[9], S A Asimov[13], S K Badyal[5], E Basova[12], K B Bhalla[4], A Bhasin[5], R A Bondarenkov[12], T H Burnett[11], X Cai[14], L P Chernova[13], M M Chernyavsky[9], B Dressel[8], E M Friedlander[2], S I Gadzhieva[13], E R Ganssauge[8], S Garpman[6], S G Gerassimov[9], A Gill[4], J Grote[11], K G Gulamov[13], V G Gulyamov[12], V K Gupta[5], S Hackel[8], H H Heckman[2], B Jakobsson[6], B Judek[10], F G Kadyrov[13], H Kallies[8], Y J Karant[2], S P Kharlamov[9], S Kitroo[5], J Kohli[5], G L Koul[5], V Kumar[4], P Lal[4], V G Larinova[9], P J Lindstrom[2], L S Liu[14], S Lokanathan[4], J Lord[11], N S Lukicheva[13], L K Mangotra[5], N V Maslennikova[9], E Monnand[3], S Mookerjee[4], C Mueller[8], S H Nasyrov[12], W S Nawotny[13], G I Orlova[9], I Otterlund[6], N G Peresadko[9], S Persson[6], N V Petrov[12], R Raniwala[4], S Raniwala[4], N K Rao[5], J T Rhee[8], N G Salmanova[9], W Schulz[8], F Schussler[3], V S Shukla[4], D Skelding[11], K Soderstrom[6], E Stenlund[6], R S Storey[10], J F Sun[7], M I Tretyakova[9], T P Trofimova[12], Z O Weng[7], R J Wilkes[11], G F Xu[1], P Y Zheng[1].

1) Beijing, Academica Sinica, Peoples Republic of China
2) Berkeley, Lawrence Berkeley Lab, USA
3) Grenoble, C.E.N.
4) Jaipur, University of Rajasthan, India
5) Jammu, University of Jammu, India
6) Lund, University of Lund, Sweden
7) Lingfen, Shanxi normal University, Peoples Republic of China
8) Marburg, Phillips University, West Germany
9) Moscow, Lebedev Institute, USSR
10) Ottawa, NRC, Canada
11) Seattle, Washington University, USA
12) Tashkent, Inst. Nucl. Phys., USSR
13) Tashkent, Physical-Technical Inst., USSR
14) Wuhan, Hua-Zhong normal University, Peoples Republic of China

ABSTRACT: Experiment EMU-01 makes use of emulsion chambers and conventional stacks to study the interactions in matter of 200 A GeV ^{16}O nuclei accelerated at the CERN SPS. Projectile fragmentation is compatible with such interactions of ^{16}O nuclei at 2 A GeV, indications of limiting fragmentation. Partic-

le production is examined via high precision pseudo-rapidity distributions. Energy densities up to about 3 GeV/fm^3 are observed in central ^{16}O + Ag(Br) interactions. Pseudo-rapidity density distributions and fluctuations are well reproduced by the MC model Fritiof, although the existence of new and unknown sources of density fluctuations are not excluded by the data.

INTRODUCTION: The acceleration of ^{16}O ions up to 200 A GeV at CERN and 14.6 A GeV at Brookhaven heralds a significant advance in the field of relativistic heavy ion physics. The possibility for creating in the laboratory conditions that existed in the first moments of the universe focuses much interest onto the field. Whether phase transitions can be realised or not in ^{16}O induced reactions remains an open question. None-the-less, vital to any search for the existance of a phase transition is an understanding of hadronization in the nuclear environment. This aspect of particle production is a principal aim of our experiment.

Because of the complementary nature of observations made in emulsion stacks and chambers, target and projectile fragmentation reactions at 200 A GeV can also be examined in detail and compared directly with fragmentation (spectator) reaction at lower energies. In particular, the high precision of angle measurements in emulsion chambers enables us to obtain specific information on the He (Z=2) projectile fragments (PF) from peripheral 200 A GeV ^{16}O interactions.

EMULSION DETECTORS AND MEASURING EQUIPMENT: In Nov-Dec 1986 fifty emulsion chambers, each 10*10*10 cm^3 in volume, and six emulsion stacks, up to 20 cm in length, were exposed to the CERN SPS ^{16}O beam at energies 60 A and 200 A GeV. (Similar exposures were also made at Brookhaven using the 14.6 A GeV - ^{16}O beam. To date our effort has been concentrated on the 200 A GeV irradiations.)

An emulsion chamber consists of 7 sheets of 0.8 mm thick polystyrene plastic, each coated on both sides with FUJI emulsion. The emulsion layers are 100 μm thick, except for sheet number three which was 350 μm thick and functions as the target layer. The emulsion sheets were separated by paper honey-cone structures and held in position under slight pressure in the light-tight chamber box. The chambers were exposed with the beam entering normal to the emulsion

sheets. Each chamber was irradiated at four beam spots, each approximately 2.5 cm in diameter, with intensities 2 - $6*10^3$ nuclei/cm^2. The NIKFI-emulsion stacks received single-beam exposures parallel to the 600 μm - thick emulsion pellicles at similar intensities.

The coordinates of particle tracks in the emulsion chambers and stacks are measured relative to adjacent, non-interacting beam tracks. Measuring systems are of two general types:

a) Devices that consist of a microscope with an attached optical system which superimposes the three images of the microscope image; The ordinary microscope image, the coordinate digitizing pad and the display of the monitor of the microcomputer system. These systems are especially designed for measurements in the emulsion chambers, where the coordinates of tracks are measured in each plane in a fixed field of view (~ 500 μm dia). Angle measurements are therefore limited to angles $\leq 30°$. Standard deviation in the measured emission angles is ~ 0.013 units in pseudo-rapidity, η, in the interval $1 < \eta < 7$.

b) Devices that incorporate a microscope with digital readout of the xyz stage coordinates in 1 μm units (typically). Stage travel is sufficient to fully encompass the areas of the emulsion plates (up to 10*20 cm^2). Stages can be under manual and/or computer control. Such systems are used for measurements in both emulsion stacks and chambers. With such systems, emission angles are measured to $\sigma \sim 3*10^{-5}$ rad, e.g. $\sigma(\eta) \sim 0.1 - 0.2$ at $\eta = 9$, the pseudorapidity characteristic of He projectile fragments of ^{16}O at 200 A GeV.

In both systems, the measured coordinates of all tracks (including vertex) are subjected to least squares, 3-dimensional reconstruction programs that yield the particle multiplicity and pseudo-rapidity, $\eta = -\ln(\tan \Theta/2)$, distributions on an event-by-event basis.

PROJECTILE FRAGMENTATION:

The high spatial resolution that is attained with emulsion chambers has enabled us to measure the projected angles θ_x and θ_y, and pseudo-rapidity η of the He PF's associated with the ^{16}O projectile. The angles θ_x and θ_y are the projections of the polar angle of emission of the PF's on the yz and xz planes, where z is the vector direction of the incident ion. Because θ_x and θ_y are in principle the same, we present them as a single distribution in Fig. 1. The data are based on a total of 97 interactions, giving rise to 178 He PF's with multiplicities $1 \leq N_{He} \leq 3$. In this sample no 4-He events were observed. The angular distribution is gaussian-shaped, with dispersion $\sigma(\theta_{xy}) = (21.2 \pm 1.2)*10^{-5}$ rad. Given that the incident momentum is 200 A GeV/c, the corresponding momentum is estimated to be $P_{xy} = 159 \pm 9$ MeV/c. Assuming isotropy in the projectile frame, P_{xy} is equivalent to the longitudinal momentum P_l, which permits favourable comparison of this result with $P_l = 137 \pm 2$ MeV/c observed in 2.1 A GeV ^{16}O interactions /1,2/.

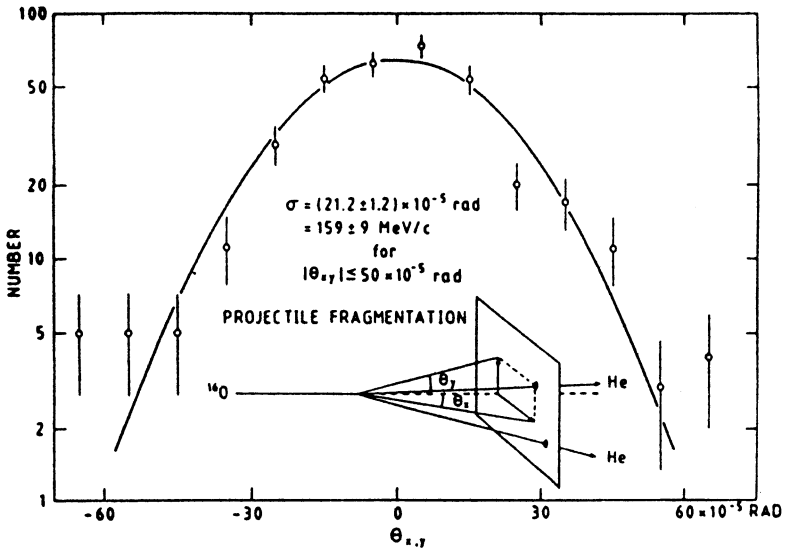

Figure 1. Projected polar angles θ_x and θ_y of the fragments. Solid curve is gaussian fitted to data, $|\theta_{xy}| \leq 50*10^{-5}$ rad.

Fig. 2 shows the momentum dispersion of the He PF's as a function of the multiplicity of the He. For each multiplicity we show the sensitivity of the evaluated dispersions on the cutoff values of P_{xy}. For the case $|P_{xy}| < 300$ MeV, the values of σ_{Pxy} can be directly compared with (unpublished) data on the dispersion of the PF's from 2.1 A GeV ^{12}C interactions obtained with the HISS facility (LBL) /3/.

Tentative conclusions are evident: i) The dispersions σ_{Pxy} of He PF's from 200 A GeV ^{16}O and 2 A GeV ^{12}C are in close agreement, indicative of energy independence. ii) This energy independence, i.e. limiting fragmentation, appears to extend to the individual multiplicity channels, with the angular dispersion of the He tending to increase with decreasing He multiplicity.

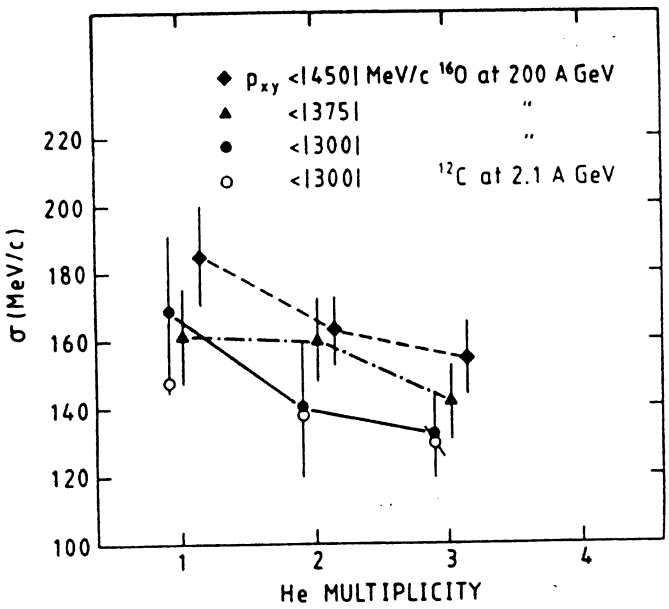

Figure 2. Dispersions of the projected angular distributions versus He multiplicity. Closed points are from this experiment, showing dependence on cut-off values. He dispersions from ^{12}C interactions at 2.1 A GeV, with $|P_{xy}| < 300$ MeV/c, are also shown.

Fig. 3 presents the emission angles of the He PF's in terms of pseudo-rapidity η. The solid curve is the predicted η-distribution based on the He spectrum measured at 2.1 A GeV (σ_{P_l} = 137 MeV/c). The observed values $\langle\eta\rangle = 9.15 \pm 0.06$ with η in the range $7.6 \leq \eta \leq 13$, are all in excellent agreement with the spectrum derived from the transformation of 2.1 A GeV data to 200 A GeV.

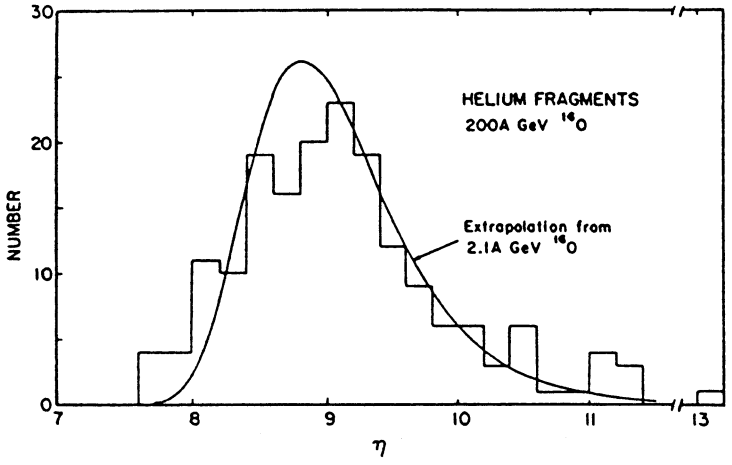

Figure 3. Pseudo-rapidity distribution of He PF's. The expected distribution extrapolated from 2.1 A GeV is indicated.

CHARGED PARTICLE PRODUCTION:

Lund Model: We shall compare the experimental data on particle production with predictions from the Lund model for high- energy nucleus-nucleus interactions /4/. This model is a generalization of the Lund hadron scattering model /5/, and incorporates the basic feature of long formation time where all cascading

is neglected. Comparisons with the data will be made by use of a reference sample of 5000 events generated by the Monte Carlo version of the Lund model called Fritiof /6/. Any restrictions that were imposed on the experimental data were likewise imposed on the reference sample.

Particle Multiplicities: In each event the pseudo-rapidities η were measured for all singly-charged, i.e. shower, particles with $\beta \geq 0.7$. The number of such particles will be denoted n_s. Event samples include one of minimum bias, and one of central events where the number of produced particles is $n_s \geq 150$. The data are dominated by measurements made in emulsion chambers, where experimental procedures permitted full acceptance of particle production only at angles $\leq 30°$ ($\eta \geq 1.3$) with respect to the beam axis. A small fraction of the data were obtained from events measured in the emulsion stacks with no angular restrictions. The multiplicity distributions of n_s observed in emulsion chambers are shown in Fig. 4. Fig. 4a shows the n_s distribution for the minimum bias sample and Fig. 4b is the distribution with $n_s >$ 150. The Lund model Fritiof predicts the n_s distributions as indicated. Except where detection efficiency are expected to be low for events with $n_s \leq 10$, the model reproduces the data fairly well. The rapid decline of the distribution for $n_s > 200$ reflects the limiting numbers of participant nucleons in the interactions of ^{16}O with Ag(Br) in the emulsion.

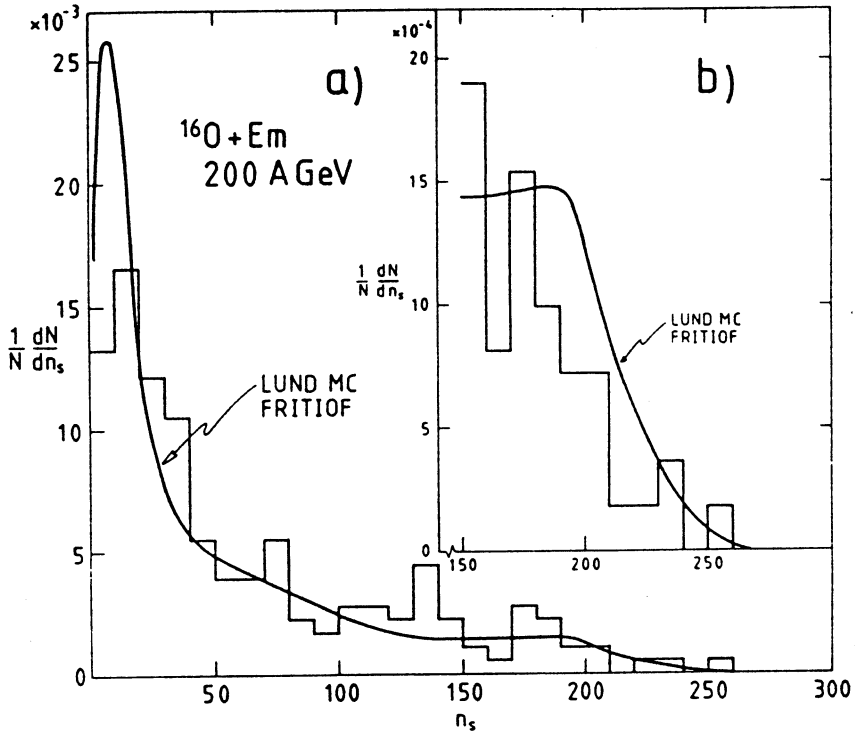

Figure 4. Multiplicity distributions for shower particles, $\beta > 0.7$ and $\theta < 30°$. a) Minimum bias, b) Central events with $n_s \geq 150$. Predictions from the Lund model Fritiof are indicated.

Particle Densities: Fig. 5 presents the average pseudo-rapidity density distributions $\rho(\eta) = N^{-1} dn/d\eta$ for three sub-samples. The distribution shown in Fig. 5a is for events with $n_s \geq 200$, which comprises about 1.5% of the total inelastic cross section. The data are compared with the density distribution corresponding to 1.5% of the Fritiof-generated events having the highest multiplicities. Likewise, the $\rho(\eta)$-distribution for events with $150 < n_s < 200$ shown in Fig. 5b comprise about 6% of the cross section, hence are compared with Fritiof of this level. Apart from the observation that the Lund model predicts mean multiplicities $\langle n_s \rangle$ that are about 10% greater than is measured for each of these distributions, the calculated and measured distributions show excellent agreement as to shape and position of the peak densities.

Fig. 5c displays the $\rho(\eta)$ distribution for peripheral events, defined as having $10 \leq n_s < 50$. In contrast to events with $n_s \geq 150$, we see here a substantial contribution of particles at very large values of η. Such particles are identified with non-interacting

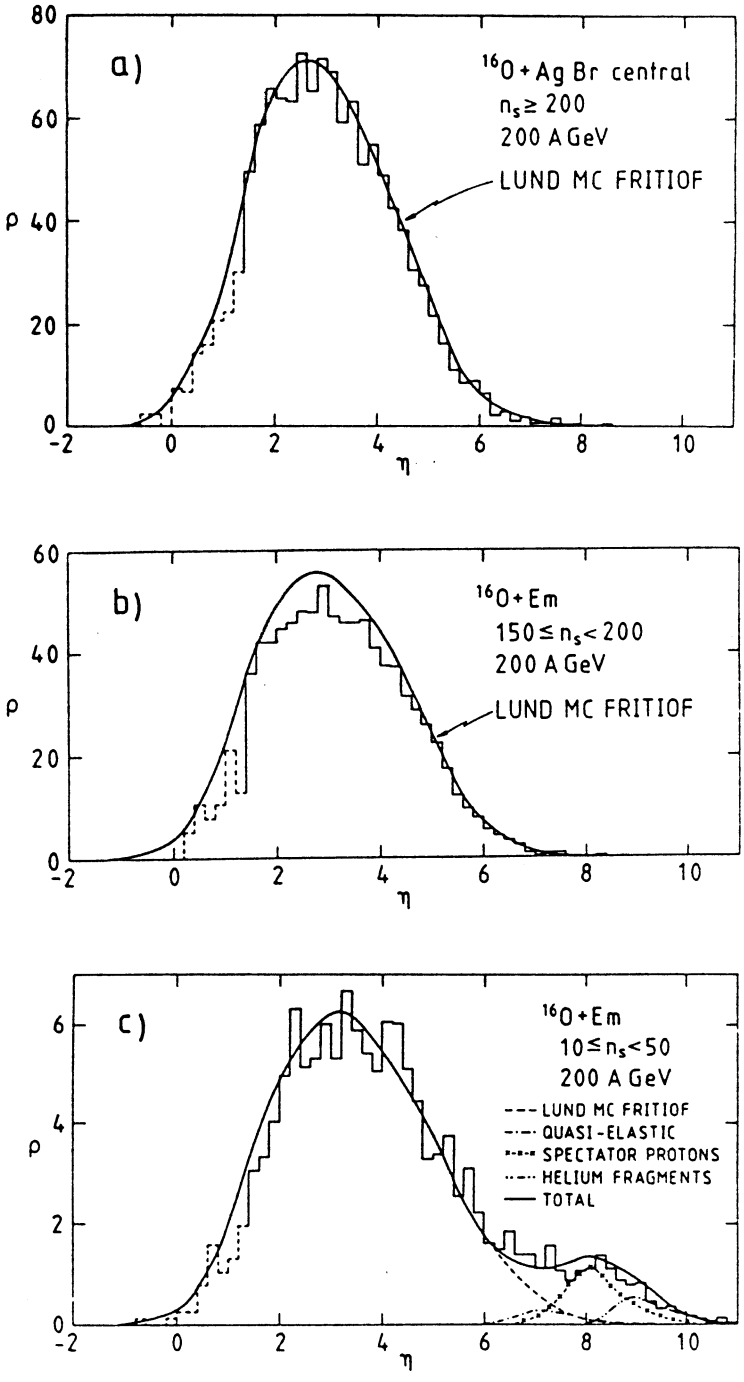

Figure 5. Pseudo-rapidity density distributions for charged particles. a) Sample of events with $n_s \geq 200$, b) with $150 \leq n_s < 200$ and c) with $10 \leq n_s < 50$.

"spectator" fragments of the projectile that are emitted near beam velocity at very small angles, i.e. angles that are largely governed by Fermi motion within the fragmenting projectile. The corresponding values of η are therefore large. The contributions to the high-η values are attributed to quasi-elastic scattering, spectator protons and He nuclei, the η-spectrum of the latter having been given in Fig. 3. These three contributions to the pseudo-rapidity density spectrum, which are not included in the Lund model, can realistically account for the shape of the distribution for $\eta > 7$. It is readily apparant that the complete absence of projectile fragmentation that occurs for events having $n_s > 150$ is a valid operational criteria for the centrality of collisions between nuclei.

Density Fluctuations: Four frequency distributions of particle densities ρ observed in each unit of pseudo-rapidity in the interval $1.5 \leq \eta \leq 5.5$ for all events with $n_s \geq 150$ are presented in Fig. 6, a) through d). Each unit of η region is subdivided into bins of width $\Delta\eta = 0.2$. The distribution of particle densities in each region predicted by Fritiof are superimposed on the data. That the calculated fluctuations are in good with experiment supports arguments that the observed fluctuations have their origins in the intrinsic fluctuations attributable to the number of participating nucleons, the break-up of the excited strings, decay of resonances, etc. We point out the observations in our data sample with exceptionally high local densities (up to $p(\eta)=140$) suggest the possible existance of new sources for density fluctuations may be present in some rare type of events. Finally, we show in

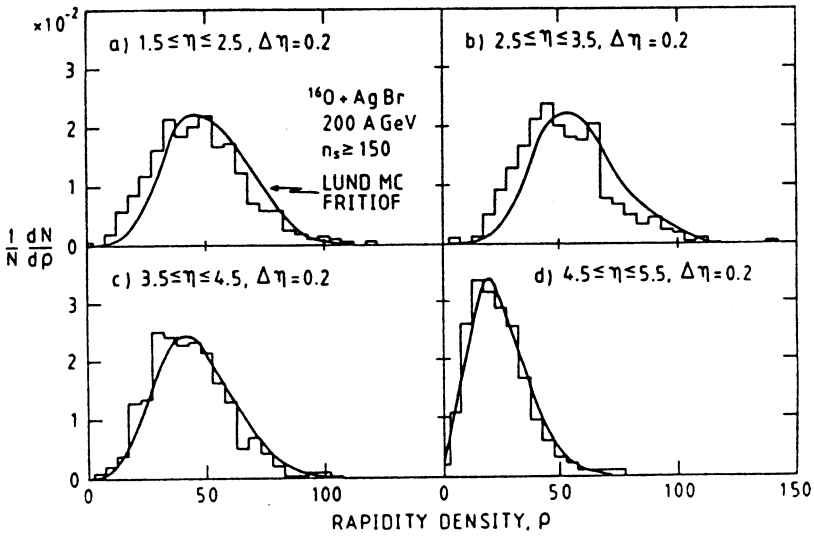

Figure 6. Particle density distributions in bins of width $\Delta\eta = 0.2$ in four different regions of η each of unit width in the interval $1.5 \leq \eta \leq 5.5$.

REFERENCES:

1. D. Greiner et al., Phys Rev Lett 35, 152(1975).
2. H. Heckman et al., Phys Rev C17, 1735(1978).
3. P. Lindstrom, private communication.
4. B. Anderson et al., Nucl Phys A447, 161c(1986).
   B. Anderson et al., Lund University Report, LU-TP 86-3(1986).
   B. Anderson et al., Physica Scripta 34, 451(1986).
5. B. Anderson et al., Phys Report 97, 31(1983).
   T. Sjöstrand, Computer Physics Com 39, 347(1986).
6. B. Nilsson-Almqvist and E. Stenlund, Computer Physics Com 43, 373(1987).
7. J.D. Bjorken, Phys Rev D27, 140(1983).

DISCUSSION:

Question: Very approximately, how many helium nuclei are produced from ^{16}O interaction? (D. Morrison)

Reply: The fragmentation of $^{16}O \rightarrow nHe$ (n = 1 to 4) occurs in about 1/3 of all interactions. On the average, about 0.6 of a He fragment is produced per interaction.

Fig. 7 the strong correlation between rapidity density and the total multiplicity n_s. The curves indicate $\langle\rho(n_s)\rangle$ given by the Lund model. The dispersion of the data about the predicted means are compatible with those obtained from the Lund model (not shown). The energy-density scale on the right is based on the Bjorken formula /7/, with $\langle p_t \rangle$ = 0.35 GeV/c. In the extreme cases, the energy densities reach values of almost 2-3 GeV/fm^3.

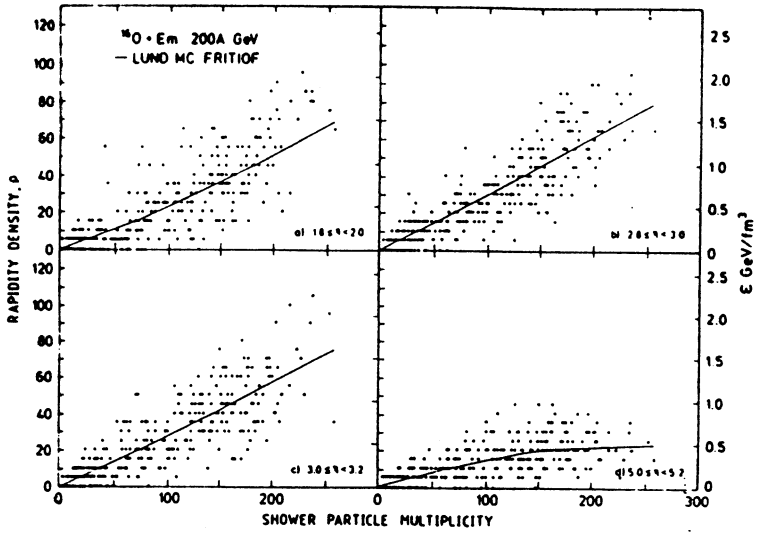

Figure 7. Particle densities versus total charged particle multiplicities for four different intervals of η. The curves give the average behavior predicted by the Lund model.

CONCLUSIONS: We succinctly summarize our results on 200 A GeV ^{16}O + Em interactions as follows: a) The processes of projectile fragmentation induced by ^{16}O at 200 A GeV are, within present statistics, the same as those observed at 2 A GeV, i.e. limiting fragmentation is satisfied. b) Particle production is well accounted for by the Lund model, Fritiof, although new and unknown sources of fluctuations are not excluded by the data.

ACKNOWLEDGEMENTS: We give kudos to the CERN staff of the PS and SPS for their outstanding performance in producing the ^{16}O beam for this experiment. Among the many persons on the CERN staff who made our experiment possible are G. Vanderhaeghe, K. Ratz, N. Dobble, P. Grafstrom, M. Reinharz, H. Sletten and J. Wotschack. We are grateful for the assistance of A. Oskarsson in monitoring the beam during the exposures of the emulsion, and, most importantly, for the contributions given by the scanning/measuring staffs within the collaboration.

This work was supported by the Director, Office of Energy Research, Division of Nuclear Physics of the Office of High Energy and Nuclear Physics of the U.S. Department of Energy under Contract DE-AC03-76SF00098.

LAWRENCE BERKELEY LABORATORY
TECHNICAL INFORMATION DEPARTMENT
UNIVERSITY OF CALIFORNIA
BERKELEY, CALIFORNIA 94720